



YIELDS FROM HIGHLY ASYMMETRIC FISSION:  
FRACTIONAL CUMULATIVE YIELDS OF  
 $^{143}\text{Ba}$ ,  $^{144}\text{Ba}$ , AND  $^{147}\text{Ce}$  FROM  
THERMAL-NEUTRON INDUCED  
FISSION OF  $^{235}\text{U}$

---

A Dissertation  
Presented to  
The Faculty of the Graduate School  
University of Missouri

---

In Partial Fulfillment  
of the Requirements for the Degree  
Doctor of Philosophy

---

by  
Nelva<sup>E.</sup> Gross Runnalls  
June 1966

David E. Troutner, Dissertation Supervisor

## ACKNOWLEDGMENTS

This research was supported by the American Association of University Women as part of their program of fellowships for American women.

The author desires to express her appreciation to her advisor, Dr. David E. Troutner, for suggesting the problem and for his continuing guidance and encouragement. She also wishes to thank Dr. Robert L. Ferguson for assistance in the work done at the Oak Ridge National Laboratory and for his advice and suggestions during the course of the work. To Mr. Donald Hastings, who assisted with several of the fast separations, sincere thanks are also given.

2397c

## TABLE OF CONTENTS

CHAPTER	PAGE
I. INTRODUCTION . . . . .	1
Postulates for Nuclear Charge Division . . .	1
Equal Charge Displacement . . . . .	1
Minimum Potential Energy Hypothesis . . .	2
Empirical $Z_p$ Function . . . . .	2
Fractional Yield Measurements . . . . .	3
II. MASS-147 CHAIN . . . . .	8
Experimental Procedures . . . . .	8
Irradiations . . . . .	9
Rapid Separation Procedures . . . . .	9
Double Precipitation Method . . . . .	10
Single Precipitation With Wash . . . . .	11
Single Precipitation With No Wash . . . . .	11
Radiochemical Purification . . . . .	12
Estimation of Experimental Error . . . . .	14
Sample Preparation and Radioactivity	
Measurements . . . . .	14
Calculations . . . . .	15
Calculation of the $^{147}\text{Ce}$ Yield and	
Half-Life . . . . .	17
III. MASS-143 CHAIN . . . . .	21
Experimental Procedures . . . . .	21

CHAPTER	PAGE
Irradiations . . . . .	21
Rapid Separation Procedure . . . . .	22
Decontamination of Cerium . . . . .	22
Radioactivity Measurements . . . . .	24
Calculations . . . . .	25
Corrections for Incomplete Separation . . . . .	27
Calculation of $^{143}\text{Ba}$ Yield and Half-Life . . . . .	28
Yield of $^{143}\text{Cs}$ . . . . .	32
IV. MASS-144 CHAIN . . . . .	34
Experimental Procedures . . . . .	34
Radioactivity Measurements . . . . .	34
Calculations . . . . .	36
V. DISCUSSION . . . . .	40
Isobaric Charge Dispersion . . . . .	46
Variation of $Z_p$ With Mass Number . . . . .	51
Half-Life of $^{144}\text{Ba}$ . . . . .	56
VI. SUMMARY . . . . .	57
BIBLIOGRAPHY . . . . .	59

## LIST OF FIGURES

FIGURE	PAGE
1. Mass-143, mass-144, and mass-147 beta-decay chains . . . . .	7
2. The fraction of mass-147 chain present as $^{147}\text{Ce}$ as a function of separation time . . .	19
3. Fast-separation apparatus . . . . .	23
4. The fraction of mass-143 chain present as $^{143}\text{Ba}$ as a function of separation time . . .	29
5. The fraction of mass-144 chain present as $^{144}\text{Ba}$ as a function of separation time . . .	37
6. Gaussian plots of mass-143 and mass-144 nuclear charge dispersions . . . . .	41
7. Probability plot of measured fractional cumulative yields for masses 95, 140, 141, and 143 as a function of $(Z - Z_p + \frac{1}{2})/\sigma$ . .	43
8. Nuclear charge dispersion probability plot for mass 143 . . . . .	44
9. Nuclear charge dispersion probability plot for mass 144 . . . . .	45
10. Known values of $\sigma$ in the mass 139-144 region plotted as a function of A . . . . .	47
11. Known values of $\sigma$ plotted as a function of A' .	50
12. $^{235}\text{U}$ ( $n_{\text{th}}$ , F) empirical $Z_p$ values . . . . .	53

## LIST OF TABLES

TABLE	PAGE
I. Fraction of Mass-147 Chain Present as $^{147}\text{Ce}$ at Separation Time . . . . .	20
II. Fraction of Mass-143 Chain Present as $^{143}\text{Ba}$ at Separation Time . . . . .	30
III. Fraction of Mass-144 Chain Present as $^{144}\text{Ba}$ at Separation Time . . . . .	38
IV. Average Number of Neutrons in Fission Fragments With the Most Probable Charge (Product Masses 133-139) . . . . .	52

## CHAPTER I

### INTRODUCTION

The several hypotheses advanced to describe distribution of charge in low energy fission processes have two objectives; (a) prediction of  $Z_p$ , the most probable charge for a given mass, and (b) prediction of the width of the distribution around this most probable charge. Halpern (1) reviewed proposals made before 1959, and Coryell, Kaplan and Fink (2) reviewed those presented before 1960.

#### I. POSTULATES FOR NUCLEAR CHARGE DIVISION

##### Equal Charge Displacement

The hypothesis of equal charge displacement (ECD) proposed by Glendenin, Coryell, and Edwards (3) is in agreement with the gross features of experimental observations. They postulated that the most probable fission mode leads to equal chain lengths for complementary fission products (the term products is applied to fragments after emission of prompt neutrons). That is,

$$Z_{A_1} - Z_{P_1} = Z_{A_h} - Z_{P_h}$$

where  $Z_A$  is the most stable charge for the given mass, and subscripts h and l refer to the heavy and light fragments respectively.

Pappas (4) modified this postulate by applying the equal chain lengths rule to fragments before prompt neutron emission. Several different methods for estimating  $Z_A$  have been used, and the predicted  $Z_p$  values depend on the choice of method (2). Fiedler and Herrmann (5), using a new mass surface formula, have reported predictions in agreement with measured independent yields.

#### Minimum Potential Energy Hypothesis

Blann, quoting Swiatecki (6), proposed that the most probable division of charge minimizes the combined coulombic and potential energy of the fissioning nucleus. This proposal, known as the minimum potential energy hypothesis (MPE), requires estimation of masses of nuclides far removed from stability and is thus largely dependent on the choice of mass formula for making these estimates.

Coryell (2) found the ECD and MPE hypotheses give similar results in the mass region for which most data are available, provided the same mass formula is used in estimating  $Z_A$  for both.

#### Empirical $Z_p$ Function

A method for predicting  $Z_p$  which is independent of estimates of  $Z_A$  was derived by Wahl et al. (7). At the time of Wahl's work, the  $Z_p$  values for six mass numbers, all in the region of high fission yields, were known empirically,



since two or more independent yields had been measured for each of these mass numbers. Since the width of the charge distribution varied only slightly for these six mass numbers, Wahl and his co-workers assumed the charge dispersion measured for these mass numbers was generally applicable. Values of  $Z_p$  for mass numbers for which a single independent yield had been measured were calculated on this basis, and an empirical  $Z_p$  function derived.

## II. FRACTIONAL YIELD MEASUREMENTS

Radiochemical methods are suitable for experimental observations of charge division in the fission process because the radioactivity of most fission products allows very small quantities to be detected and identified by these sensitive methods, and because one member of an isobaric decay chain, being a different element from the other members, may be separated by chemical means for observation of its independent yield. The fraction of those fission events which result in products of a given mass number which are produced as one nuclide of that mass is known as the fractional independent yield of that nuclide. The fractional cumulative yield of this nuclide is the sum of its independent yield and the independent yields of its precursors in the isobaric chain.

The comparison of experimentally observed primary yields with those predicted by the postulates for nuclear charge division is the usual technique for assessing the validity of these postulates. The lack of independent yield measurements for mass numbers of low fission yield prevents comparison except for high-yield mass numbers. For these mass numbers with high fission yields, where most of the measured independent yields are found, Wahl's empirical curve provides a satisfactory basis for predicting and correlating the independent yields. The shape of the empirical curve is poorly defined for mass numbers on the wings of the mass yield curve, however, because of the scarcity of measured independent yields for these mass numbers.

Wolfsberg (8) has found that for mass numbers produced in high yield, the most probable charge of the light fragment is  $\sim 0.6$  charge units higher than would be found if the proton-to-neutron ratio in each fragment remained the same as that in the fissioning nucleus. This suggests the distribution of charge in the fission process concentrates the charge in the light mass fragment. This effect is also evidenced in Wolfsberg's data for thermal-neutron induced fission of  $^{233}\text{U}$  and  $^{239}\text{Pu}$ , and 14-MeV neutron induced fission of  $^{235}\text{U}$  and  $^{239}\text{Pu}$ . There are not enough data available for mass numbers produced in low yields to show

whether this effect continues for these mass numbers.

Thus, extending the measurement of independent fission yields to include mass numbers outside the area of high yields became desirable. To obtain more information on charge distribution for an isobaric chain of a heavy mass number, the present work was undertaken to measure the fractional cumulative yield of  $^{147}\text{Ce}$  in thermal-neutron fission of  $^{235}\text{U}$ .

Recently, Niece (9) measured the independent yield of  $^{95}\text{Zr}$ . This result, in combination with the previously measured fractional yields of  $^{95}\text{Kr}$  and  $^{95}\text{Y}$ , showed the dispersion of charge about  $Z_p$  for the mass-95 chain differs from that predicted by Wahl on the basis of measurements in the peak yield region. Niece postulated a systematic decrease in the width of the charge dispersion with increasing fission product mass, and constructed an empirical function for predicting the width of charge distribution for a given mass.

In the light of these findings, measurement of a second independent yield in a heavy mass chain, to allow measurement of the width of charge distribution in this region, became of interest.

In the course of the  $^{147}\text{Ce}$  experiments, a method for purifying and assaying fission product cerium had been adapted for use in estimating completeness of removal of

cerium from praseodymium in the fast separation.

This method of assaying fission-product cerium was used in connection with a rapid separation of fission-product lanthanum from its barium precursor to allow measurement of the fractional cumulative yields of  $^{143}\text{Ba}$  and  $^{144}\text{Ba}$ . Previous measurements of two independent yields (Xe and Ce) in the mass-143 chain, and of one yield (Xe) in the mass-144 chain had been reported. An additional fractional yield in each of these chains allows calculation of the width of charge distribution for the 144 chain, re-examines that previously reported for the 143 chain, and tests the Gaussian shape of the dispersion for mass 143.

Figure 1 represents the isobaric chains considered in this study; the half-lives are those reported at the time the work was undertaken, and are taken from the compilation by Herrmann (10).

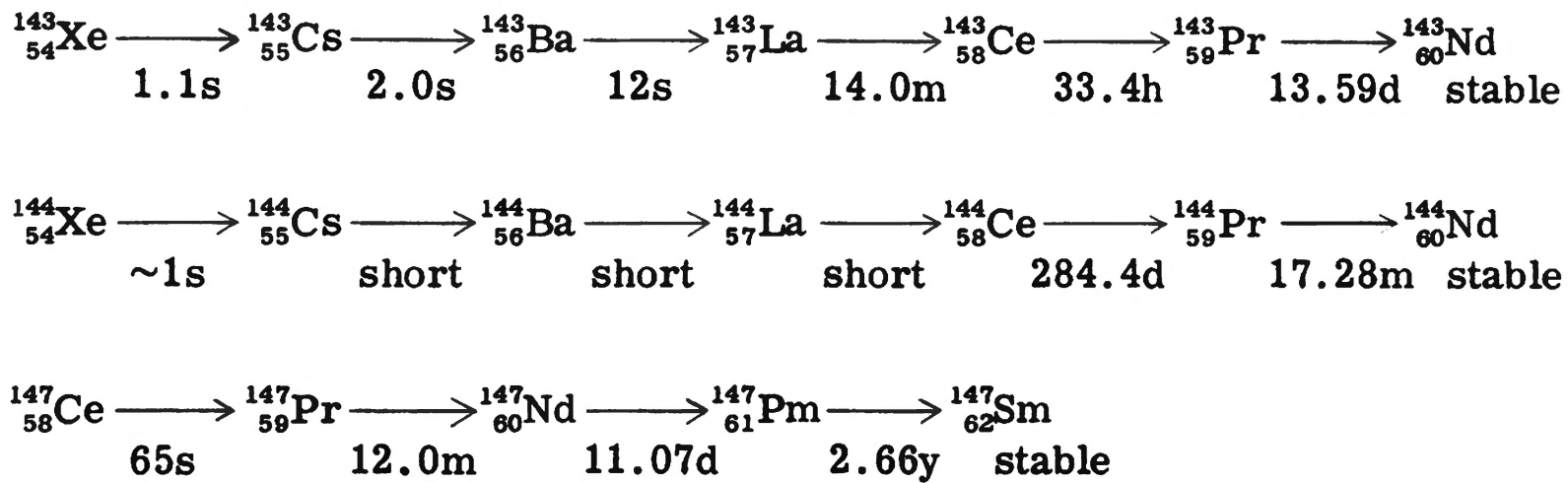


Figure 1. Mass-143, mass-144, and mass-147 beta-decay chains.

## CHAPTER II

### MASS-147 CHAIN

#### I. EXPERIMENTAL PROCEDURES

The fractional cumulative yield of  $^{147}\text{Ce}$  was measured in a series of nine experiments. Each experiment consisted of a brief irradiation of a uranium solution, followed by a rapid chemical separation of fission-product cerium from its daughter praseodymium and the other lanthanides in part of the irradiated solution. Two samples were obtained from each separation: the untreated part of the irradiated solution, and the filtrate from the rapid precipitation procedure. After a delay to allow shorter-lived members of the mass-147 chain to decay to the  $^{147}\text{Nd}$  daughter, neodymium was purified from the other fission product activities and assayed radiochemically in each sample. By comparison of the specific activities of  $^{147}\text{Nd}$  in the two samples, the fraction of the decay chain existing as  $^{147}\text{Ce}$  at the time of the initial separation was calculated. The results of a series of such irradiations, followed by separations at gradually increasing time intervals, were used to calculate the fraction of the total chain existing as  $^{147}\text{Ce}$  at the time of irradiation.

### Irradiations

Irradiations were made in the pneumatic tube facility of the Oak Ridge Research Reactor. The sample containers were cylindrical polyethylene "rabbits" with a capacity of approximately one ml. The conventional thermal-neutron flux inside the rabbit at the irradiation position was estimated to be  $6 \times 10^{13}$  neutrons  $\text{cm}^{-2} \text{sec}^{-1}$ . The ratio of  $^{235}\text{U}$  fissions produced in the absence of a cadmium absorber to the fissions produced in the presence of a cadmium absorber was not measured in this work. The ratio had been shown previously (9) to be about 55.

Each irradiated solution consisted of 100  $\mu\text{g}$  of  $^{235}\text{U}$  (95 per cent enriched) as  $\text{U}_3\text{O}_8$  dissolved in  $\sim 1$  ml of dilute nitric acid. The duration of each irradiation was 10 seconds.

### Rapid Separation Procedures

Separation of cerium from praseodymium and other lanthanides was accomplished by precipitation of  $\text{Ce}(\text{IO}_3)_4$  and vacuum filtration through a fritted-glass filtering funnel. A total of nine separations was made by the following methods. For all three methods of precipitation, all solutions containing  $\text{KBrO}_3$  were warmed on a hot water bath and cooled to room temperature immediately before use, to ensure oxidation of the cerium to the +4 oxidation state.

All frits were treated with a suspension of filteraid and drained shortly before use.

Double precipitation method. After a 10-second irradiation, the rabbit was impaled by a hollow needle and the contents drawn by vacuum through the needle into a solution containing 2 ml of 10-mg/ml  $\text{Ce}^{4+}$ , 1 ml of 10-mg/ml  $\text{Nd}^{3+}$ , and 2 ml of concentrated  $\text{HNO}_3$ ; the entire solution having been saturated with  $\text{KBrO}_3$ . Approximately half of this solution was drained into a 30-mm medium-porosity fritted-glass funnel on which was suspended 0.16 g  $\text{I}_2\text{O}_5$  dissolved in 1 ml of the 10-mg/ml suspension of filteraid. After mixing for  $\sim 10$  seconds, the solution was vacuum filtered. The filtrate was drained into a second fritted-glass funnel on which was suspended a solution of 1 ml of 10-mg/ml  $\text{Ce}^{4+}$ , 0.5 ml of concentrated  $\text{HNO}_3$ , and 0.3 ml of  $\text{H}_2\text{O}$ , all saturated with  $\text{KBrO}_3$ ; and the solution again filtered.

Tracer experiments showed that less than 0.5 per cent of the cerium remained in the filtrate after the second precipitation. For each precipitation, the following times were recorded: beginning and end of irradiation, precipitation, beginning and end of first filtration, and beginning and end of second filtration. The time of separation was taken as the precipitation time.

The neodymium carrier was used in the fast separation to act as a carrier for the praseodymium fission



products; tracer experiments showed that in this precipitation neodymium does act as a carrier for praseodymium.

Single precipitation with wash. The rabbit contents were transferred to a solution containing 1 ml of 20-mg/ml  $\text{Ce}^{4+}$ , 1 ml of 10-mg/ml  $\text{Nd}^{3+}$ , both in 5 M  $\text{HNO}_3$ , all saturated with  $\text{KBrO}_3$ . Approximately half of this solution was drained into a fritted-glass filtering funnel on which was suspended  $\sim 5$  ml of 5 M  $\text{HNO}_3$  saturated with  $\text{I}_2\text{O}_5$ . After the solution had been mixed for 10 seconds, the precipitate was removed by vacuum filtration and washed with 5 ml of the precipitating reagent. The following times were recorded: beginning and end of irradiation, precipitation, beginning and end of filtration, and beginning and end of wash.

Tracer experiments showed  $2.8 \pm 1.7$  per cent of the cerium present at the time of precipitation in the filtrate under these conditions, and that  $3.8 \pm 0.6$  per cent of the cerium was deposited in the filtrate by the wash solution. Corrections for this amount of contamination were applied to measurements made by this method.

Single precipitation with no wash. The conditions were identical to those in the method immediately above except that the wash was omitted. The values were corrected for  $2.8 \pm 1.7$  per cent of the cerium present at the time of separation.

### Radiochemical Purification

To each fraction from the rapid separation, (the filtrate and the portion of the solution remaining in the mixing vessel into which the irradiated solution was drawn), 1 ml of a 10-mg/ml barium holdback carrier solution was added, and  $\text{Nd}(\text{OH})_3$  was precipitated with concentrated  $\text{NH}_4\text{OH}$ . The solutions were centrifuged, and the  $\text{Nd}(\text{OH})_3$  washed. The samples were sent to the University of Missouri at Columbia in this form.

Upon arrival at Columbia, each sample was further purified by addition of cerium carrier and reprecipitation of the iodate. The supernatant liquid and washings from this precipitation were combined and further purified by the method described by Bunney *et al.* (11).

In this procedure, additional barium holdback carrier is added, and the rare earth hydroxides are centrifuged from solution after addition of  $\text{NH}_4\text{OH}$ . The hydroxide precipitate is washed, then dissolved in concentrated HCl and passed through an ion exchange column (bed dimensions  $\sim 50$  cm x 1 cm x 1 cm) containing Dowex 2X8 anion exchange resin, 50-60 mesh. The rare earths are eluted with concentrated HCl. The cycle of hydroxide precipitation and ion exchange purification is repeated two additional times, with NaOH used instead of  $\text{NH}_4\text{OH}$  for the final hydroxide precipitation. The rare earth hydroxides are then dissolved in a minimum

of concentrated HCl, evaporated to dryness under an infrared lamp, and taken up in 500  $\mu$ l of 0.02 N HCl.

Neodymium was then purified from the total rare earth fraction by the method described by Rengan and Meinke (12), in which the solution containing the rare earths is loaded on a micro ion-exchange column containing Dowex 50X12, -400 mesh, and eluted under pressure with a 0.2 M solution of  $\alpha$ -hydroxy isobutyric acid in which the pH has been adjusted to 5.08 with  $\text{NH}_4\text{OH}$ .

Elution of the neodymium fraction as a function of drop number was determined by tracer experiments with  $^{147}\text{Nd}$ .

The neodymium fraction was collected, and  $\text{Nd}(\text{OH})_3$  precipitated with  $\text{NH}_4\text{OH}$ . The  $\text{Nd}(\text{OH})_3$  was centrifuged from solution, then dissolved in a minimum of concentrated HCl. The two samples which resulted from portions of one irradiated solution were diluted to equal volumes and aliquots taken for counting and for measurement of the neodymium concentration.

The spectrophotometric method described by Rinehart (13) was used to measure the neodymium concentration. Each sample was analyzed at the time of purification, and again from aliquots of the sample used for assay of the radioactivity after the  $^{147}\text{Nd}$  had decayed. The final analyses were made in triplicate. The results of the initial and final analyses were in agreement.

### Estimation of Experimental Error

Multiple determinations of the concentration of a labeled neodymium solution spectrophotometrically and radiochemically showed that the spectrophotometric procedure has a relative error of 0.392 per cent in four determinations, while the radiochemical measurement had an error of 0.622 per cent in four determinations. Values obtained for the specific activity by the combined radiochemical and spectrophotometric methods in four dilutions of one solution showed a relative error of 1.29 per cent.

To test the efficiency of the purification and the reproducibility of the results for a mixture of fission products, a solution of irradiated  $^{235}\text{U}$  in which  $6 \times 10^{10}$  fissions had been produced was added to 15 mg of neodymium carrier, and three aliquots were purified by the method described. The relative error in the specific activities measured for the three aliquots was 0.775 per cent.

### Sample Preparation and Radioactivity Measurements

Decay of the  $^{147}\text{Nd}$  was followed for five or more half-lives by single-channel gamma spectrometry. The detector was a 1 x 1 inch thallium-activated sodium iodide well crystal. The 5-ml liquid samples were contained in Pyrex counting tubes. Variations in counter efficiency became significant because of the low energy of the  $^{147}\text{Nd}$  radiation and the long time intervals during which the

measurements were made. The effect of these fluctuations on the measured specific activity ratio was minimized by considering the ratio of activities of each pair of samples on a given day as one measurement of this ratio and finding the mean value of these ratios for all of the measurements. Significant absorption effects of the glass counting tubes on the measured activities were shown to be absent as follows. After radioactivity measurements for all the samples had been completed, 5-ml aliquots of a  $^{147}\text{Nd}$  solution were pipetted into the cleaned counting tubes from each experiment, and the activity measured in the way described above. No statistically significant variations in activity were observed.

## II. CALCULATIONS

The experiment results in a measurement of the ratio of atoms present as  $^{147}\text{Pr}$  and  $^{147}\text{La}$  at the time of separation to the total number of atoms of mass 147 produced in the irradiation. This ratio is called  $Q$  for convenience. In each experiment, two samples were obtained. In the B sample, which resulted from the portion of the solution not subjected to the rapid separation procedure, the neodymium activity represented all of the mass-147 chain. The A sample was obtained from the filtrate after precipitation of ceric iodate; in this sample the neodymium

activity was reduced by the amount which would have grown from the cerium removed in the rapid separation procedure.

Two measurements were made for each pair of samples: the ratio of  $^{147}\text{Nd}$  activities at a given time, (A/B), and the ratio of neodymium concentrations after dilution to equal volumes,  $[A]/[B]$ . From these values,  $Q$  was calculated as follows.

Let  $n_1$ ,  $n_2$ , and  $n_3$  represent the yields of  $^{147}\text{La}$ ,  $^{147}\text{Ce}$  and  $^{147}\text{Pr}$  respectively, expressed as atoms present at the time of separation. If  $j$  mg of neodymium carrier is added to the irradiated uranium solution, there are present in the B sample  $[(n_1 + n_2 + n_3)/j]$  atoms of mass 147/mg Nd. In the other aliquot of the solution, the A sample, the rapid precipitation of cerium left in the solution  $[(n_1 + n_3)/j]$  atoms of mass 147/mg Nd.

Let  $k$  = mg of Nd recovered from sample A

$i$  = mg of Nd recovered from sample B

$\epsilon$  = efficiency of the counting procedure,  
which was the same for samples A and B

$\lambda$  = decay constant for  $^{147}\text{Nd}$

Then the activity of the A sample, corrected for decay to the time of separation, is

$$[(n_1 + n_3)/j] k \epsilon \lambda$$

The activity of the B sample, corrected to the time of separation, is

$$[(n_1 + n_2 + n_3)/j] i \epsilon \lambda$$

The ratio of the activity of the A sample to the B sample is

$$\frac{[(n_1 + n_3)/j]_{k \in \lambda}}{[(n_1 + n_2 + n_3)/j]_{i \in \lambda}}$$

Simplifying, the ratio of activities in the two samples, (A/B), is

$$\left[ \frac{(n_1 + n_3)}{(n_1 + n_2 + n_3)} \right] (k/i)$$

The ratio of concentrations of neodymium in equal dilutions of the two samples, which was measured spectrophotometrically, is equivalent to the ratio (k/i). Thus

$$\begin{aligned} (A/B) \quad [B]/[A] &= (n_1 + n_3)/(n_1 + n_2 + n_3) = Q \\ (1 - Q) &= n_2/(n_1 + n_2 + n_3) \end{aligned}$$

The quantity, (1 - Q), represents the fraction of the  $^{147}$  chain present as cerium at the time of separation.

#### Calculation of the $^{147}$ Ce Yield and Half-Life

The values for the fraction of the chain present as cerium are plotted on a logarithmic scale as a linear function of the separation time in Figure 2. The measured values and separation times are reported in Table I. Since the fraction which exists as cerium decreases with time because of the decay of  $^{147}$ Ce, this plot is analogous to the usual plot of the decay of a radioactive substance. A line fit to the experimental points by an unweighted least-squares calculation results in a half-life of  $78 \begin{smallmatrix} +9 \\ -7 \end{smallmatrix}$  seconds for  $^{147}$ Ce, in agreement with the half-life of  $65 \pm 6$  seconds

previously reported by Hoffman and Daniels (14). The intercept, representing the fraction of the mass-147 chain present as cerium at the mean irradiation time, is  $0.963 \pm 0.063$ . The error in measuring Q was estimated to be  $\pm 5$  per cent. The error in  $(1 - Q)$  produced by this error was calculated and is shown in Table I and Figure 2. The least squares calculation and the calculation of error limits are described by Youden (15).



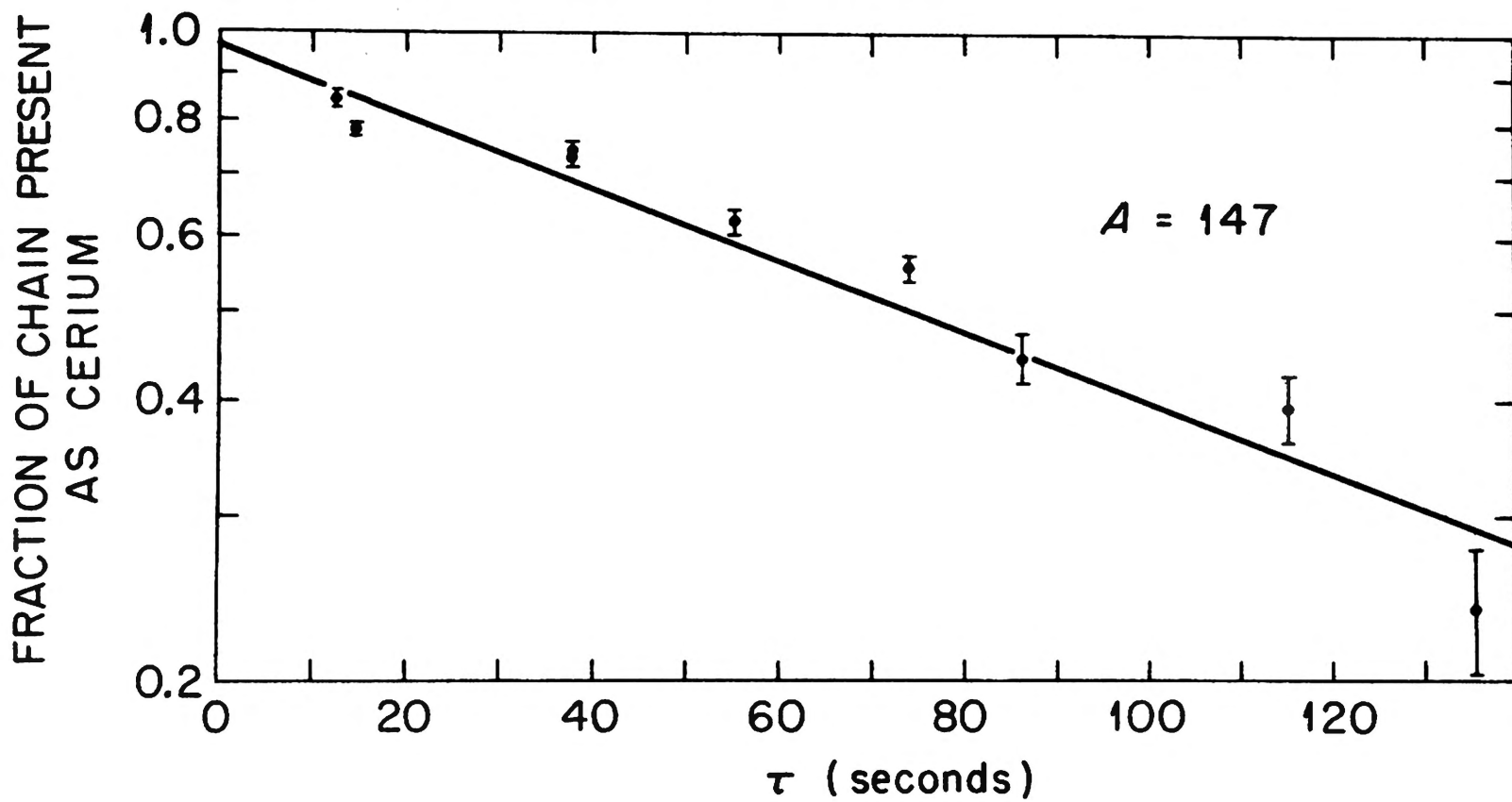


Figure 2. The fraction of mass-147 chain present as  $^{147}\text{Ce}$  as a function of separation time.

TABLE I

FRACTION OF MASS-147 CHAIN PRESENT  
AS  $^{147}\text{Ce}$  AT SEPARATION TIME

<u>Precipitation Time</u> (seconds)	<u>(1 - Q)</u>
12.30	$0.844 \pm 0.008$
14.39	$0.781 \pm 0.011$
30.79	$0.744 \pm 0.013$
30.83	$0.781 \pm 0.013$
55.13	$0.625 \pm 0.019$
74.04	$0.560 \pm 0.022$
86.10	$0.448 \pm 0.028$
115.04	$0.396 \pm 0.030$
135.37	$0.240 \pm 0.038$

## CHAPTER III

### MASS-143 CHAIN

#### I. EXPERIMENTAL PROCEDURES

The experiments which measured the independent yield of  $^{143}\text{La}$  were similar in design to those already described for the mass-147 chain: a short irradiation, rapid chemical separation, and radiochemical purification and assay of a daughter product. In this case, the elements to be separated were barium and lanthanum; this was accomplished by quickly precipitating lanthanum hydroxide from the irradiated solution. After the shorter-lived members of the mass-143 chain had decayed to  $^{143}\text{Ce}$ , equal amounts of cerium carrier were added to the precipitated  $\text{La}(\text{OH})_3$  and to the filtrate, and cerium was purified from both solutions. By comparison of the specific activities of the  $^{143}\text{Ce}$  in the two solutions, the fraction of the mass-143 chain existing as  $^{143}\text{Ba}$  at the time of separation was calculated. From the results of a series of such irradiations, with the separations occurring at varying time intervals, the fraction of the total chain existing as  $^{143}\text{Ba}$  at the time of irradiation was calculated.

#### Irradiations

Irradiations were done at the Oak Ridge Research Reactor, as described for the experiments on the mass-147

chain, except that the duration of each irradiation was two seconds. Each irradiated solution contained 1 mg of  $^{235}\text{U}$  (95 per cent enriched) and 2 mg of natural lanthanum.

#### Rapid Separation Procedure

After the desired time interval following irradiation, each rabbit was opened by the hollow needle of the pneumatic assembly and approximately half of the contents drawn through the needle to a mixture of 4 ml of concentrated  $\text{NH}_4\text{OH}$  and 1 ml of 10-mg/ml barium carrier suspended on a 60-mm medium-porosity fritted-glass filtering funnel. The apparatus is shown in Figure 3. Each funnel was rinsed with barium carrier before use. The reactant mixture was vacuum filtered and washed with  $\sim 25$  ml of water containing 20 mg of barium and 1 ml of concentrated  $\text{NH}_4\text{OH}$ . The following times were recorded for each separation: beginning and end of irradiation, precipitation of  $\text{La}(\text{OH})_3$ , beginning and end of filtration, and beginning of wash.

#### Decontamination of Cerium

Equal aliquots of a 4-mg/ml  $\text{Ce}^{4+}$  carrier solution were added to the filtrate and to the filter funnel. The  $\text{La}(\text{OH})_3$  was dissolved from the filter with  $\text{HNO}_3$ . Each solution was made ammoniacal and the mixed lanthanum and cerium hydroxides centrifuged from solution. The hydroxides were dissolved in  $\text{HNO}_3$  and the solution made 5 N in  $\text{HNO}_3$ ,

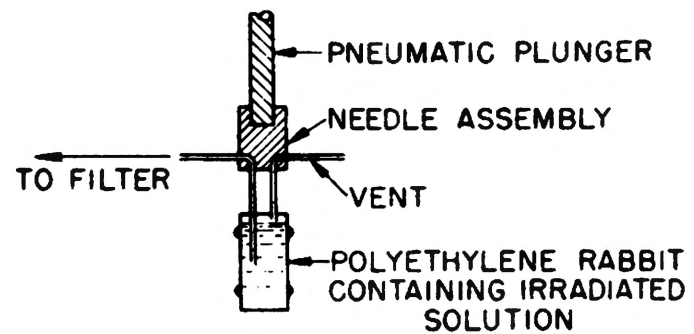
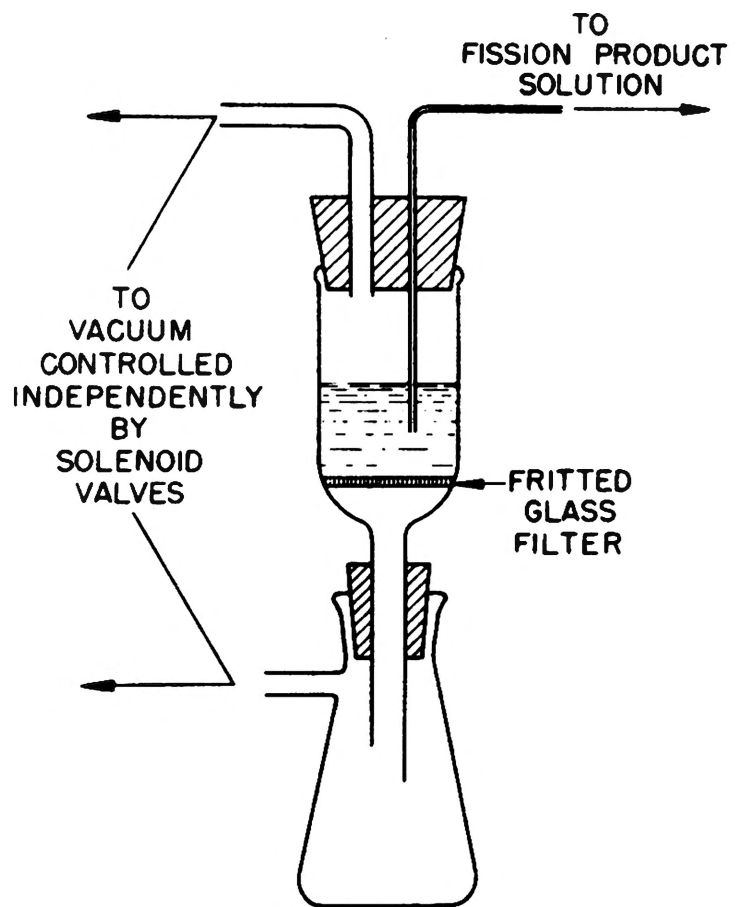


Figure 3. Fast-separation apparatus.

and the cerium oxidized to  $\text{Ce}^{4+}$  by adding solid  $\text{NaBrO}_3$  and warming on a hot water bath. To the warm solution, 1.5 ml of 5 N  $\text{HNO}_3$  saturated with  $\text{I}_2\text{O}_5$  was added. The  $\text{Ce}(\text{IO}_3)_4$  was then dissolved in concentrated  $\text{HCl}$  and transferred to polyethylene bottles for shipment to the University of Missouri at Columbia.

At Columbia, each sample was transferred to a centrifuge tube with additional concentrated  $\text{HCl}$ , and the solution heated until it became clear. The solution was made ammoniacal and the precipitated  $\text{Ce}(\text{OH})_3$  centrifuged, washed twice with water, and finally dissolved in concentrated  $\text{HNO}_3$ . The cerium was then oxidized to the +4 state and extracted into 50 ml of methylisobutyl ketone, (4-methyl-2-pentanone), back extracted into water after reduction to the +3 state, precipitated as cerous oxalate, weighed to measure relative chemical yield, and mounted for counting in that form. This procedure is described in detail by Glendenin et al. (16).

## II. RADIOACTIVITY MEASUREMENTS

Decay of the 33-hour  $^{143}\text{Ce}$  was followed in some pairs of samples by counting with a thin-window Geiger-Mueller tube, followed by resolution of the decay curves; and in the others with a single-channel gamma spectrometer, set to discriminate against other cerium fission product activities. The decay was followed for seven half-lives.

The complex decay curves resulting from the first counting method were resolved graphically into components representing 33.4-hour  $^{143}\text{Ce}$ , 13.7-day  $^{143}\text{Pr}$ , 32.5-day  $^{141}\text{Ce}$ , and 285-day  $^{144}\text{Ce}$ , by successive subtractions of the longer-lived activities.

Decay curves obtained from the gamma spectrometer consisted of the 33.4-hour activity and a longer-lived component which contributed about one per cent of the total activity. The contribution of  $^{144}\text{Ce}$  to this longer-lived component was shown by use of a  $^{144}\text{Ce}$  standard to be about 0.5 per cent. Three standards containing  $^{143}\text{Ce}$  were prepared by the method of purification described for the samples and their decay followed in the usual way. The standards showed that  $^{143}\text{Pr}$  contributed about 0.25 per cent of the initial activity of  $^{143}\text{Ce}$  to an apparent longer-lived component. Therefore, identification of the long-lived activity was considered to be satisfactory within the accuracy of the counting procedure, and it was subtracted from the decay curve.

### III. CALCULATIONS

Each separation thus resulted in two samples: one obtained from the filtrate in the fast separation (the A sample), and another which was obtained from the lanthanum hydroxide precipitate (the B sample). Short-lived members

of the mass-143 chain had decayed to  $^{143}\text{Ce}$  in both samples. The activity of the A sample resulted from cerium grown from cesium and from barium present at the time of separation, while the activity of the B sample resulted from cerium grown from lanthanum and cerium present at the time of separation. The separation time was taken to be the mean time of filtration. Addition of equal aliquots of the same cerium carrier solution to both samples leads to the following simple relationship:

- $j$  = mg of cerium added to each of a pair of samples
- $a$  = specific activity (counts  $\text{min}^{-1}/\text{mg}$  Ce recovered) of A sample at time  $t$  after irradiation
- $b$  = specific activity (counts  $\text{min}^{-1}/\text{mg}$  Ce recovered) of B sample at time  $t$  after irradiation
- $a_j + b_j$  = total activity of the chain at time  $t$
- $a_j/(a_j + b_j) = Q$  = fraction of the chain present as cesium and barium at separation time.

Simplifying,

$$Q = a/(a + b) = 1/(1 + b/a)$$

The actual quantity measured was  $b/a$ , the ratio of specific activities of the B sample to the A sample at a given time after irradiation.

In the calculation of error limits, an error of  $\pm 5$  per cent was arbitrarily assumed in the measurement of the  $b/a$  ratio. This was considered a reasonable estimate for errors in weighing, statistical errors in the counting data, and errors in resolution of the decay curves.



### Corrections for Incomplete Separation

To measure the amount of lanthanum remaining in the filtrate after the lanthanum hydroxide precipitation, in two experiments the fast separation was delayed for about two minutes after irradiation. Since essentially all the  $^{143}\text{Cs}$  and  $^{143}\text{Ba}$  had decayed by the time of separation, the  $^{143}\text{Ce}$  activity in the A sample represented lanthanum contamination of the filtrate. The amount of lanthanum in the filtrate was found to be 0.4 per cent of the lanthanum present.

The amount of barium coprecipitated with the lanthanum was measured by substituting a lanthanum carrier solution containing  $^{133}\text{Ba}$  for the rabbit contents in three fast separations, which were in all other respects identical to actual experiments. Distribution of the  $^{133}\text{Ba}$  between the filtrate and the precipitate was measured by assaying  $\text{BaCO}_3$  precipitated from each fraction of the solution. The fraction of barium found coprecipitated with the lanthanum was 1.1 per cent.

The measured Q values were accordingly corrected as follows:

$\alpha$  = fraction of chain existing as Ba at separation time

$\beta$  = fraction of chain existing as La at separation time

$$Q = \frac{\alpha - 0.011\alpha + 0.004\beta}{(\alpha - 0.011\alpha + 0.004\beta) + (\beta - 0.004\beta + 0.011\alpha)}$$

$$\alpha + \beta = 1$$

$$\alpha = (Q - 0.004)/0.985$$

### Calculation of $^{143}\text{Ba}$ Yield and Half-Life

The corrected values for the fraction of the chain present as barium and cesium are plotted on a logarithmic scale as a linear function of the separation time in Figure 4, and are tabulated in Table II. Since the fraction which exists as barium decreases with time only because of the decay of  $^{143}\text{Ba}$ , this plot is analogous to the usual plot of the decay of a radioactive substance. A line fit to the experimental points by a standard unweighted least squares calculation results in a half-life of  $13.2 \pm 0.3$  seconds for  $^{143}\text{Ba}$ . The least squares calculation and the calculation of error limits are described by Youden (15). The standard deviation of each measured point is 6 per cent, which indicates the arbitrarily assigned 5 per cent error in the b/a ratio is not unreasonable.

The intercept with the ordinate represents the fraction of the mass-143 chain present as barium at the mean irradiation time. To calculate the fractional cumulative yield of barium, it is necessary to correct this measured fraction for the yield of  $^{143}\text{Cs}$ . This correction is necessary because the barium present at any time is the sum of that produced independently as barium, which is

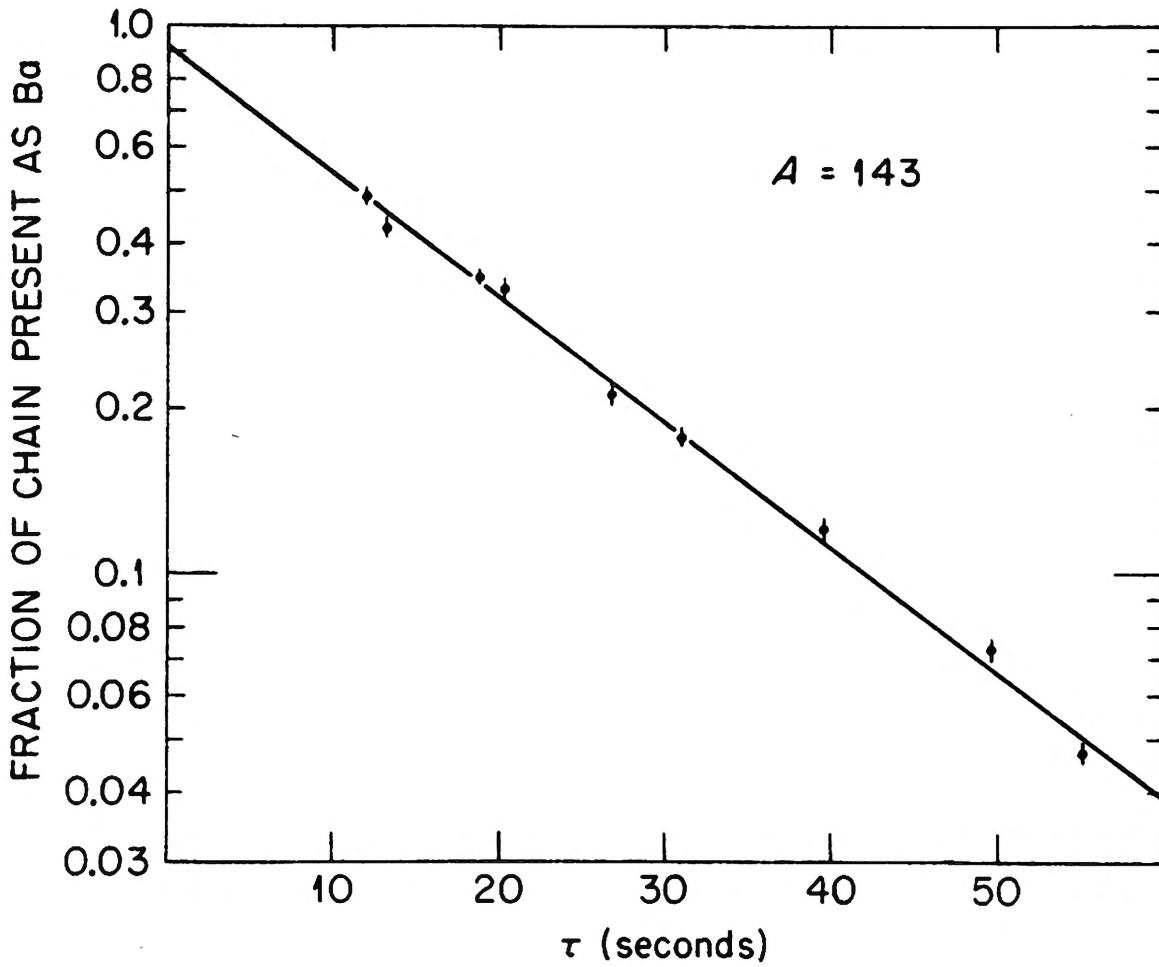


Figure 4. The fraction of mass-143 chain present as  $^{143}\text{Ba}$  as a function of separation time.

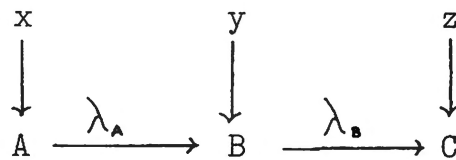
TABLE II

FRACTION OF MASS-143 CHAIN PRESENT  
AS  $^{143}\text{Ba}$  AT SEPARATION TIME

<u>Separation Time</u> <u>(seconds)</u>	<u>Fraction Present as <math>^{143}\text{Ba}</math></u>
12.03	0.492
13.34	0.432
18.94	0.349
20.34	0.335
26.80	0.212
31.00	0.179
39.54	0.121
49.68	0.073
55.10	0.047

decaying with the half-life characteristic of  $^{143}\text{Ba}$ , and of the barium which has grown from cesium originally present. The short, but finite, half-life of  $^{143}\text{Cs}$  causes the fraction of the chain present as barium, extrapolated to the mean irradiation time, to be more than the cumulative yield of barium by a small factor.

Consider the fission-product decay chain:



Let A = cesium, B = barium, C = lanthanum

x = independent yield of cesium, expressed as a fraction of total chain yield

y = independent yield of barium, expressed as a fraction of total chain yield

z = independent yield of lanthanum, expressed as a fraction of total chain yield

$\mathcal{T}$  = time in seconds from mean irradiation time to mean filtration time of fast separation

$\alpha$  = fraction of chain present as barium at time  $\mathcal{T}$

From the Bateman equations for radioactive decay (17),

$$\alpha = \left[ \frac{\lambda_A}{\lambda_B - \lambda_A} x \right] \exp -\lambda_A \mathcal{T} + \left[ \frac{\lambda_A}{\lambda_A - \lambda_B} x + y \right] \exp -\lambda_B \mathcal{T}$$

If the half-life of A is short compared to  $\mathcal{T}$  (that is,  $\lambda_A$  is large),  $e^{-\lambda_A \mathcal{T}}$  becomes small and the first term becomes

negligible compared to the second. Then

$$\alpha = \left[ \frac{\lambda_A}{\lambda_A - \lambda_B} x + y \right] \exp - \lambda_B \tau$$

$$x + y + z = 1$$

$$\alpha = \left[ \left( \frac{\lambda_A}{\lambda_A - \lambda_B} x \right) + 1 - z - x \right] \exp - \lambda_B \tau$$

$$\alpha = \left[ 1 - z + x \left( \frac{\lambda_B}{\lambda_A - \lambda_B} \right) \right] \exp - \lambda_B \tau$$

The cumulative yield of barium is  $(1 - z)$ . Thus a plot of  $\alpha$  on a logarithmic scale as a linear function of separation time results in an intercept greater than the cumulative yield of barium by the factor  $\left[ x \left( \frac{\lambda_B}{\lambda_A - \lambda_B} \right) \right]$ .

In order to evaluate this factor for the mass-143 chain, it is necessary to know, in addition to the half-life of  $^{143}\text{Ba}$  calculated above, the fractional yield and half-life of  $^{143}\text{Cs}$ .

Yield of  $^{143}\text{Cs}$

An experimental evaluation of the effect of the cesium independent yield on the measurement was obtained in the following way. In two fast separations, 1 ml of a

1 mg/ml cesium carrier solution, 1 ml of saturated  $\text{Na}_2\text{CrO}_4$  solution, and 5 ml of concentrated ammonium hydroxide solution were suspended on the filtering funnel. A basic chromate solution was used to wash the precipitate. The fast separation was otherwise unchanged from that described previously. This precipitation removed barium as well as the rare earths from solution; thus the  $^{143}\text{Ce}$  activity in the A sample represented  $^{143}\text{Cs}$  present at the separation time.

The efficiency of this precipitation for removing barium and the rare earths from solution was measured in two series of tracer experiments. Triplicate precipitations labeled with  $^{133}\text{Ba}$  showed  $0.02 \pm 0.02$  per cent of the barium present in the filtrate, and triplicate precipitations in which the rare earths were labeled with  $^{144}\text{Ce}$  in the +3 oxidation state showed  $0.2 \pm 0.2$  per cent of the rare earths present in the filtrate. The measured fractions of the chain present as  $^{143}\text{Cs}$  were corrected accordingly in each of the two experiments.

The fraction of the chain present as  $^{143}\text{Cs}$  found in these experiments is consistent with the previously reported half-life of 2.0 sec (10) and with an independent yield of 23 per cent for cesium. This is the yield predicted from a Gaussian distribution fit to the known fractional yields for the 143-mass chain. Using these values, the fractional cumulative yield of  $^{143}\text{Ba}$  is calculated to be  $0.874 \pm 0.040$ .

## CHAPTER IV

### MASS-144 CHAIN

#### I. EXPERIMENTAL PROCEDURES

The measurement of the fractional yield of  $^{144}\text{Ba}$  was a result of the same series of experiments described for the mass-143 chain. The rapid lanthanum hydroxide precipitation separated not only  $^{143}\text{La}$ , but also all other fission-product lanthanum nuclides from their precursors. The irradiations, rapid separation procedure, and decontamination of the cerium have been described in Chapter III. After the decay of  $^{143}\text{Ce}$ , the  $^{144}\text{Ce}$  activity in the same samples was assayed. From the ratio of specific activities of the B and the A samples of each pair, the fraction of the chain existing as  $^{144}\text{Ba}$  at the time of separation was calculated by the same method used for the mass-143 chain.

#### II. RADIOACTIVITY MEASUREMENTS

A continuous-flow thin-window Geiger-Mueller counter was used for assay of the  $^{144}\text{Ce}$  activity. The 2.98-MeV beta radiation from 17.3-min  $^{144}\text{Pr}$ , in equilibrium with  $^{144}\text{Ce}$ , was counted through a 214-mg/cm<sup>2</sup> aluminum absorber to discriminate against the less energetic  $^{141}\text{Ce}$  and  $^{143}\text{Pr}$  beta radiations. Three weeks elapsed between irradiation and the earliest activity measurements included



in the calculations; this delay prevented interference from the  $^{143}\text{Ce}$  gamma radiation. For each pair of samples, calculation of the activity ratio was made on the basis of four or five separate measurements. The effect of differences in counter efficiency was minimized by considering the ratio of activities of each pair of samples on a given day as one measurement of this ratio and finding the mean value for all the measurements. In each individual measurement, the statistical standard deviation was one per cent for both the sample count and the background count. However, the long counting intervals required by the low activity levels probably caused indeterminate errors in the activity measurement greater than the calculated standard deviation.

The 285-day half-life of  $^{144}\text{Ce}$  made following the decay of the samples, as proof of radiochemical purity, impractical. The lack of short-lived interferences in the  $^{143}\text{Ce}$  measurement and decay curve resolution does not prove the absence of a long-lived contaminant; it has some significance, however, since most long-lived fission products are isotopes of short-lived nuclides also produced by fission.

In order to test the decontamination procedure, three aliquots of a cerium carrier solution labeled with  $^{235}\text{U}$  fission products were purified by this procedure. Decay curves were followed with both a Geiger-Mueller tube

and by single-channel gamma-spectrometry. After decay of the short-lived species, each sample was removed from the planchet, and the cerous oxalate dissolved in acid and reprecipitated. The specific activities of the three samples agreed to within 0.35 per cent before recrystallization and were unchanged by recrystallization. This experiment showed the procedure described results in a radiochemically pure cerium sample with a reproducibly measured specific activity.

### III. CALCULATIONS

The fraction of the mass-144 chain present as barium and cesium at the time of separation was calculated for each pair of samples as described for the mass-143 chain. Corrections for incomplete separations were identical for both chains. The corrected values for the fraction of the mass-144 chain present as barium and cesium are plotted on a logarithmic scale as a linear function of the separation time in Figure 5, and are tabulated in Table III. A line fit to the experimental points by the unweighted least squares calculation described by Youden (15) results in a half-life of  $11.9 \pm 0.3$  seconds for  $^{144}\text{Ba}$ .

Calculation of the fractional cumulative yield of a nuclide from the fraction of the chain present as this nuclide at mean irradiation time is described in Chapter III. Because the half-life of  $^{144}\text{Cs}$  is unreported, the barium

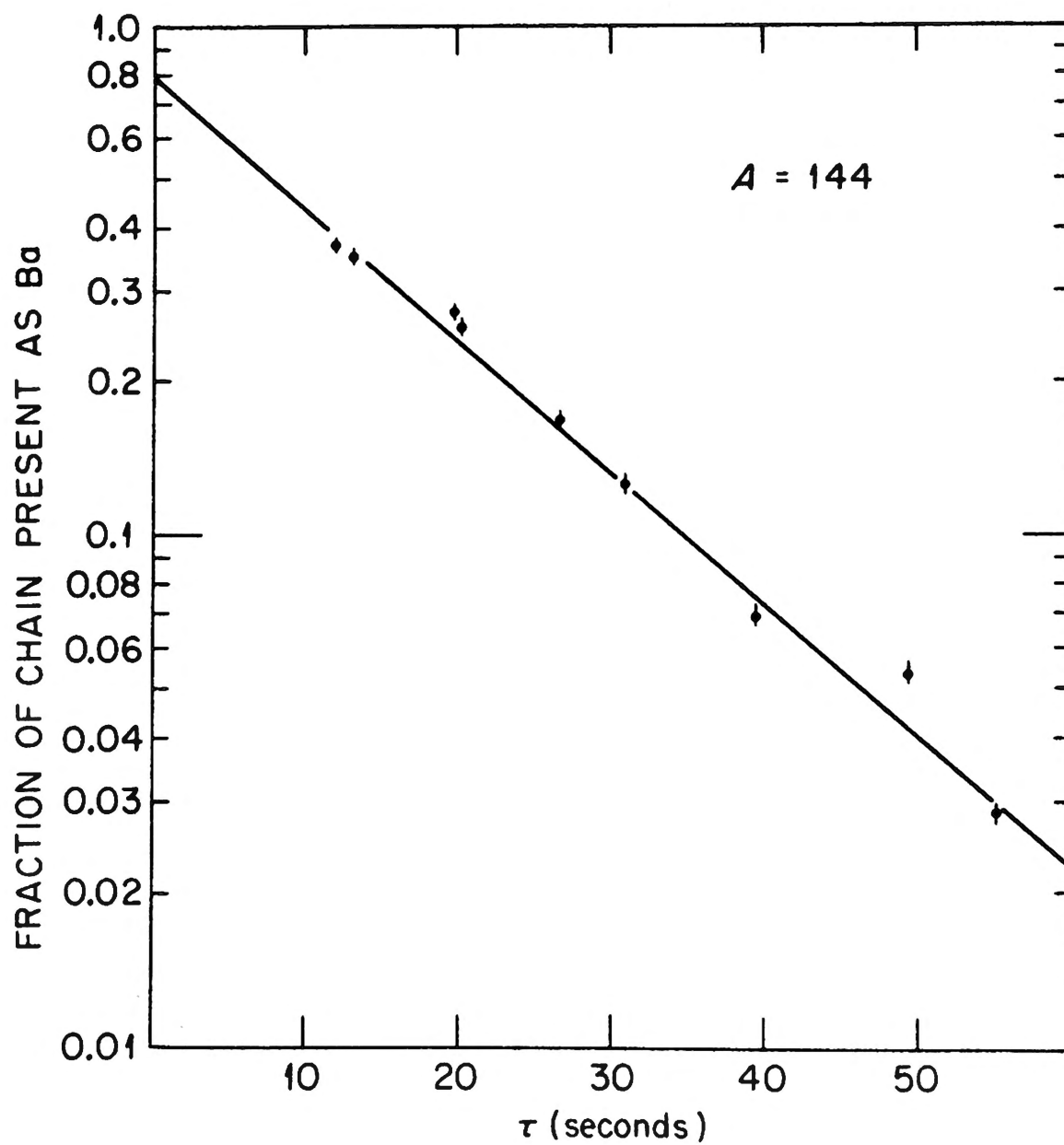


Figure 5. The fraction of mass-144 chain present as  $^{144}\text{Ba}$  as a function of separation time.

TABLE III

FRACTION OF MASS-144 CHAIN PRESENT  
AS  $^{144}\text{Ba}$  AT SEPARATION TIME

<u>Separation Time</u> <u>(seconds)</u>	<u>Fraction Present as <math>^{144}\text{Ba}</math></u>
12.03	0.371
13.34	0.352
18.94	0.276
20.34	0.255
26.80	0.169
31.00	0.127
39.54	0.069
49.68	0.054
55.10	0.029

chromate precipitation experiments can show only that the combination of yield and half-life of  $^{144}\text{Cs}$  is consistent with the yield predicted by a Gaussian distribution fit to the two experimentally measured yields in the chain, and a half-life of approximately 2 seconds. With these assumptions, the fractional cumulative yield of  $^{144}\text{Ba}$  is found to be  $0.773 \pm 0.035$ . These error limits do not include errors in the cesium yield and half-life.

## CHAPTER V

### DISCUSSION

For comparison of experimentally measured fractional yields in an isobaric chain, the measured independent yields are plotted on a logarithmic scale as a linear function of the atomic number ( $Z$ ) of the element determined. Plots for the 143- and 144-mass chains are shown in Figure 6. In each of the isobaric chains of mass 95, 140, 141, and 143, three fractional cumulative yields have been measured. For these mass numbers, nuclear charge dispersion is represented by a Gaussian distribution. The most probable charge, ( $Z_p$ ), defined by the maximum of the curve, and the standard deviation (width parameter),  $\sigma$ , of the Gaussian distribution define unique Gaussian distributions for these chains.

Consistence with the Gaussian equation

$$\begin{aligned} \sum_0^Z (P_n) &= 1/\sigma (2\pi)^{\frac{1}{2}} \int_{-\infty}^{Z + 0.5} \exp \left[ - (n - Z_p)^2 / 2\sigma^2 \right] dn \\ &= \frac{1}{2} + \frac{1}{2} f \left[ (Z - Z_p + \frac{1}{2}) / \sigma \right] \end{aligned}$$

in which  $f(x)$  is the normal probability integral, may be shown by plotting measured fractional cumulative yields as a function of  $(Z - Z_p + \frac{1}{2})/\sigma$  on probability graph paper. Figure 7 shows the measured yields for chains of mass 95,

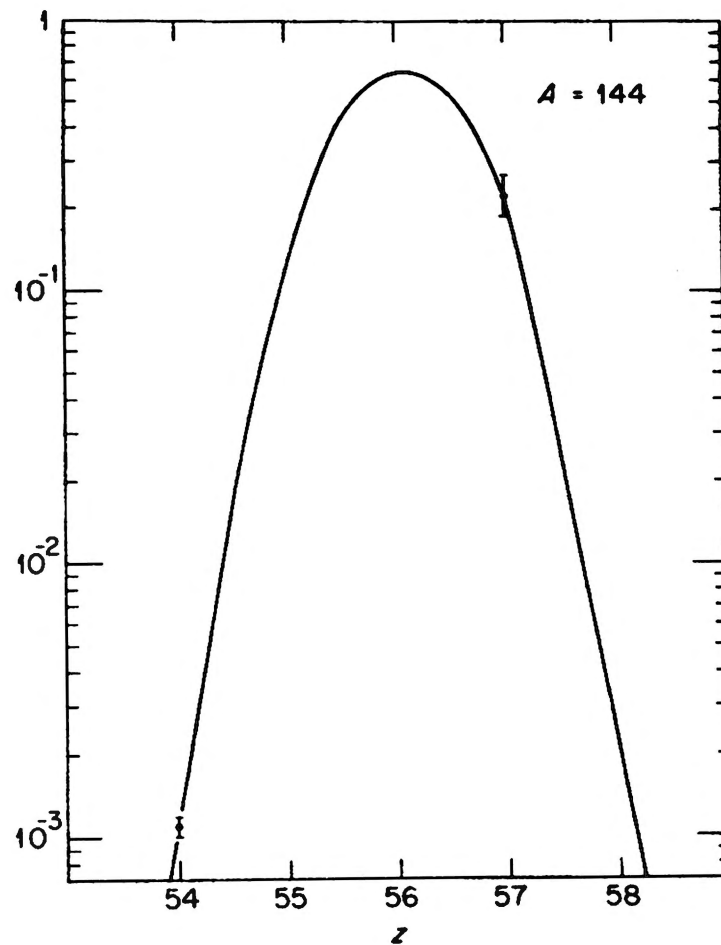
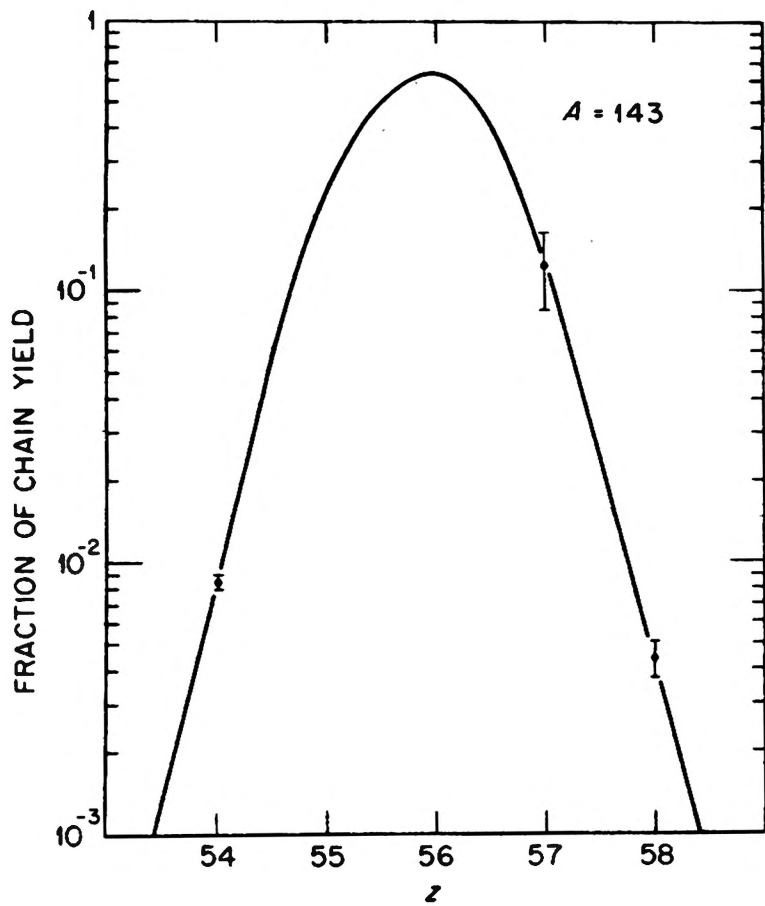


Figure 6. Gaussian plots of mass-143 and mass-144 nuclear charge dispersions.

140, 141, and 143 plotted in this way. It is evident the data are fit by the Gaussian distribution.

For a single isobaric chain, a plot of measured fractional cumulative yields may be plotted as a function of atomic number on probability graph paper, as described by Terrell (18). A Gaussian distribution appears as a straight line; from such a plot  $Z_p$  and  $\sigma$  may be obtained graphically.

Figure 8 represents such a plot for the mass-143 chain. Previously reported fractional cumulative yields;  $^{143}\text{Xe}$ ,  $8.5 \pm 0.05 \times 10^{-3}$  (7), and  $^{143}\text{La}$ ,  $0.9956 \pm 0.0030$  (7), and the fractional cumulative yield of  $^{143}\text{Ba}$  from this work are consistent with a Gaussian distribution;  $Z_p$  is  $55.92 \pm \begin{matrix} 0.08 \\ 0.10 \end{matrix}$  and  $\sigma$  is  $0.59 \pm 0.04$ .

In the mass-144 chain, one previous fractional yield is reported:  $^{144}\text{Xe}$ ,  $1.1 \times 10^{-3}$  (7). If it is assumed the charge distribution is Gaussian, two measured fractional yields provide a measure of  $\sigma$  and of  $Z_p$ . Figure 9 is a nuclear charge dispersion probability plot for mass 144. Obtained graphically,  $\sigma$  is  $0.51 \pm 0.03$  and  $Z_p$  is  $56.11 \pm 0.04$ .

Since the only experimentally measured fractional yield in the mass-147 chain is that of  $^{147}\text{Ce}$ , assumption of both a Gaussian distribution and of an arbitrary  $\sigma$  is necessary for prediction of  $Z_p$ .



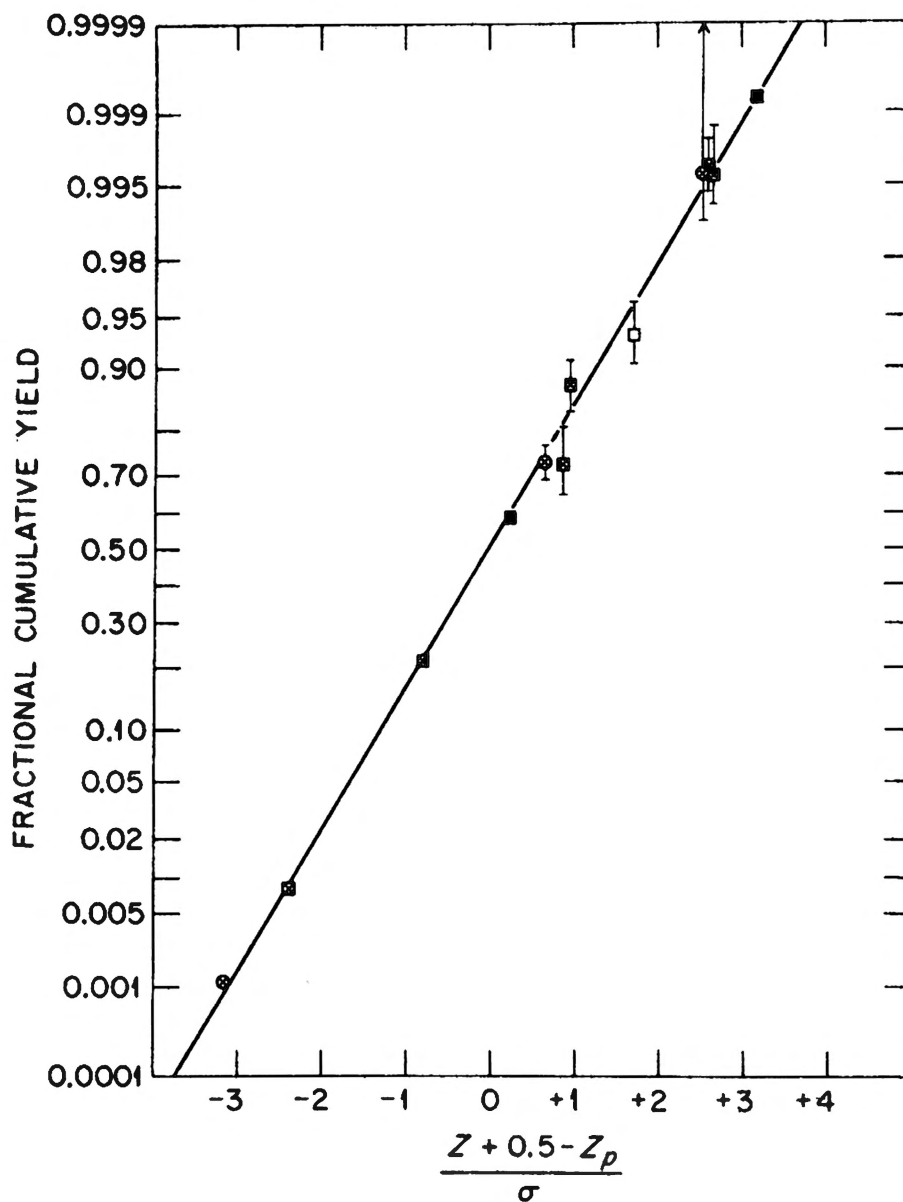


Figure 7. Probability plot of measured fractional cumulative yields for masses 95, 140, 141, and 143 as a function of  $(Z - Z_p + \frac{1}{2})/\sigma$ .

- Heavy-mass product, even-even nuclide
- Heavy-mass product, odd-odd nuclide
- ⊠ Heavy-mass product, odd A nuclide
- ⊗ Light-mass product, odd A nuclide

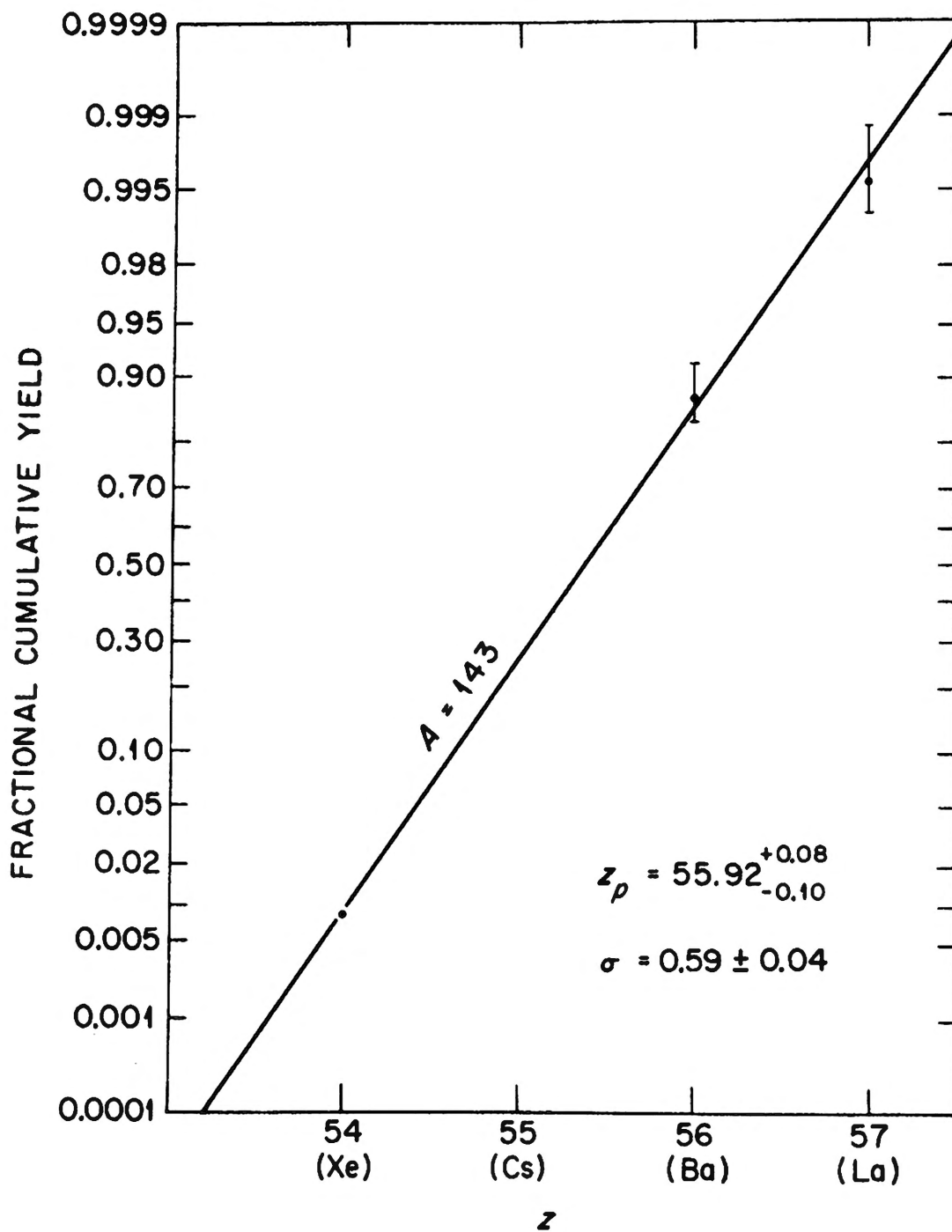


Figure 8. Nuclear charge dispersion probability plot for mass 143

$$\sigma = 0.59 \pm 0.04$$

$$z_p = 55.92 \pm \begin{matrix} 0.08 \\ 0.10 \end{matrix}$$

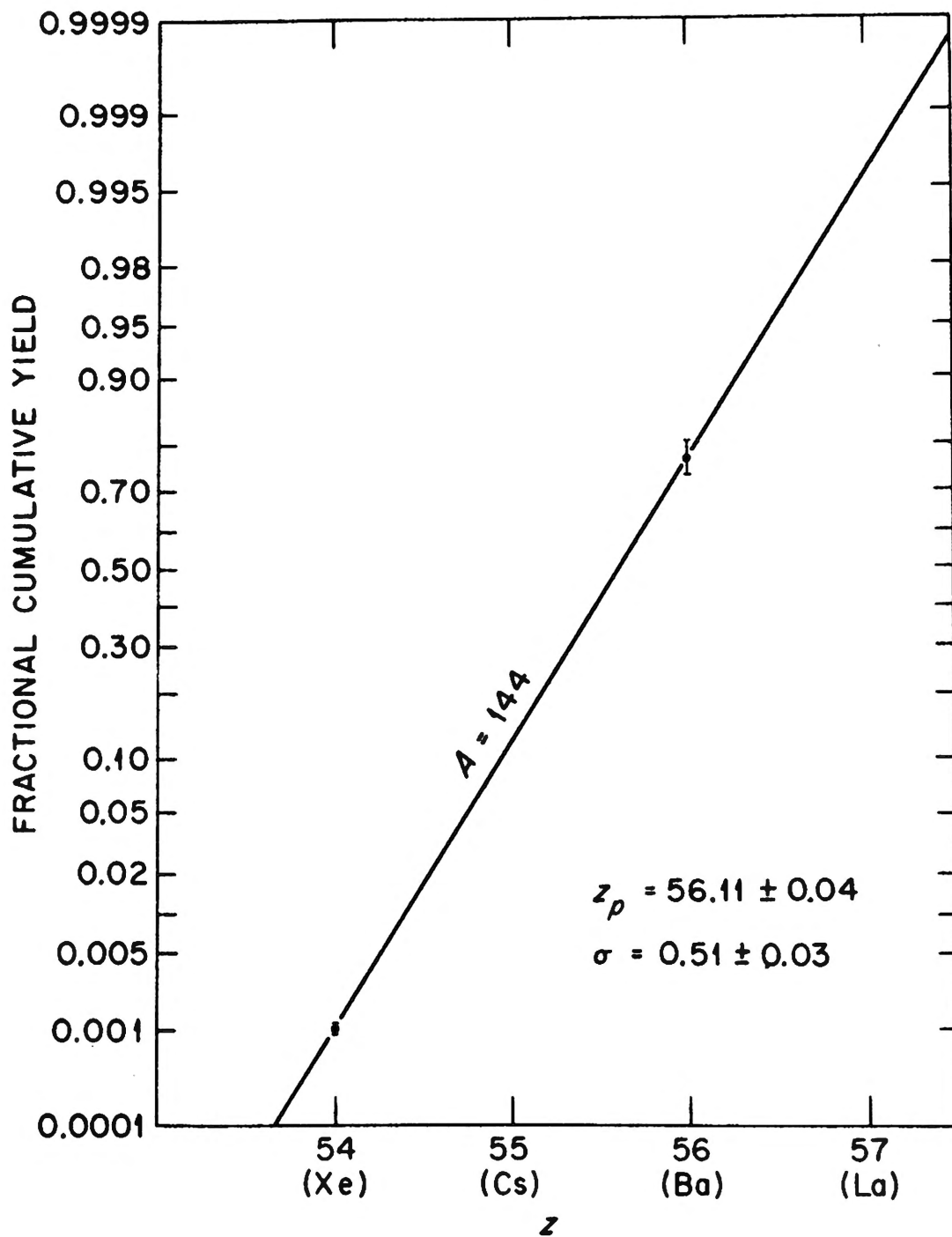


Figure 9. Nuclear charge dispersion probability plot for mass 144

$$\sigma = 0.51 \pm 0.03$$

$$z_p = 56.11 \pm 0.04$$

### Isobaric Charge Dispersion

Wahl et al. (7) assumed a  $\sigma$  of  $0.62 \pm 0.06$ , which represented the weighted average  $\sigma$  of the six uniquely defined Gaussian curves then known, to represent all isobaric charge dispersion curves. Norris (19) subsequently measured independent yields which enabled him to define  $\sigma$  for four additional isobaric chains; the new weighted average  $\sigma$  was found to be  $0.59 \pm 0.02$ . Niece (9), however, postulated that  $\sigma$  varies with mass number. Recent work by Strom et al. (20) confirms this finding.

Niece constructed an empirical  $\sigma$  function for prediction of unmeasured  $\sigma$  values by fitting a straight line to the experimental values, plotted as a function of fission product mass, for each of the fission yield peaks. The  $\sigma$  predicted for the mass-144 chain is 0.50, in agreement with the value measured in this work ( $0.51 \pm 0.03$ ).

Figure 10 shows a similar plot, in which the new  $\sigma$  value has been included. The slope, calculated by the method of least squares with each point weighted inversely as its variance, is  $-0.037 \pm 0.010$ .

Although this plot shows that  $\sigma$  varies with the fission product mass number, the suitability of assuming a linear relationship throughout the heavy mass region is questionable. The results of Strom et al. (20), who have measured  $\sigma$  values for the 131 through the 134 mass chains

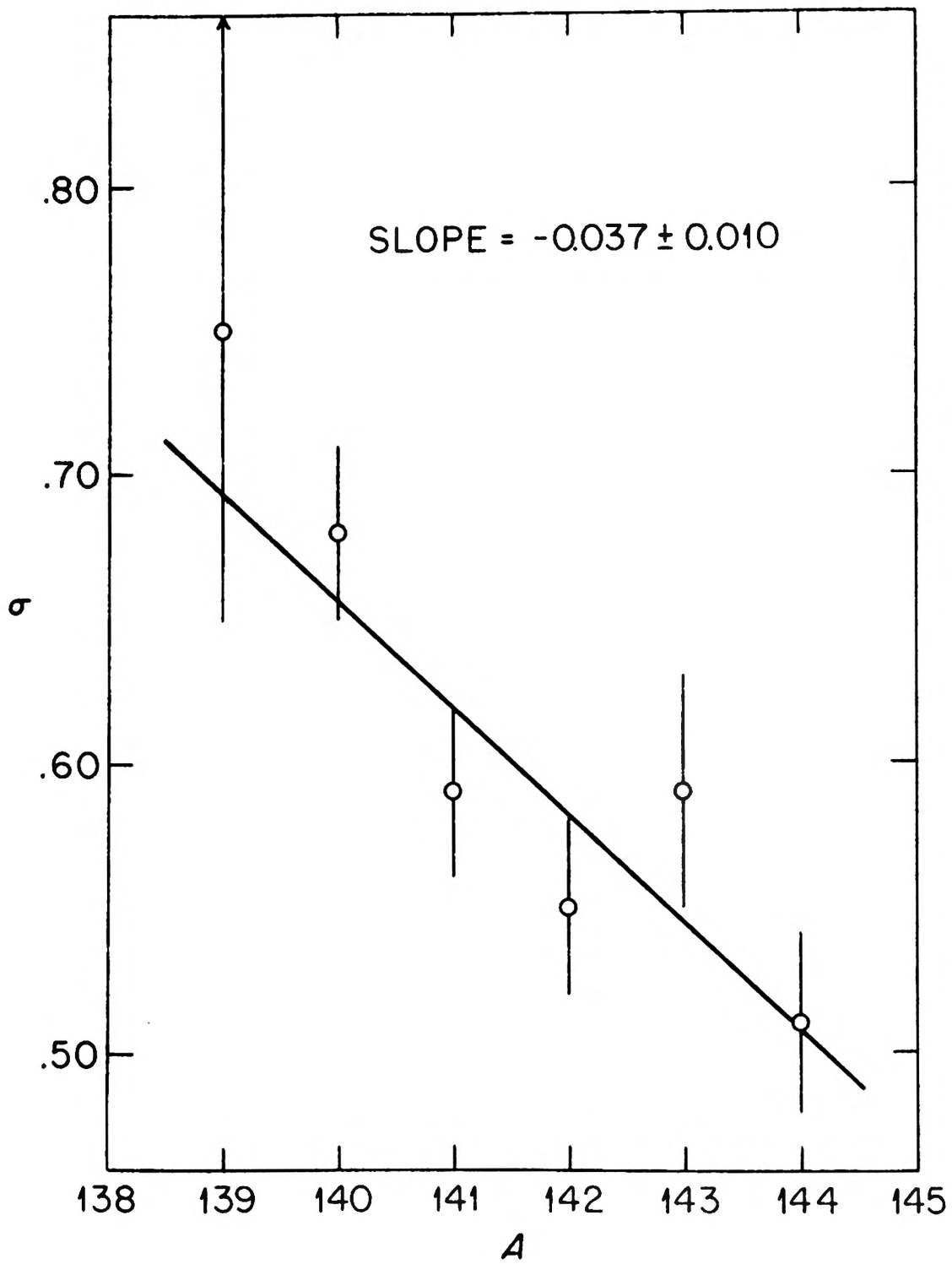


Figure 10. Known values of  $\sigma$  in 139-144 mass region plotted as a function of  $A$ .

and calculated  $\sigma$  from previously measured yields in the mass-136 chain, show a discontinuity in the values of  $\sigma$  as a function of mass number in the heavy mass region. Niece (9) found a different slope for the line of  $\sigma$  versus mass number in the light region than in the heavy region.

Radiochemical data concerning fission products are necessarily obtained as a function of the mass number of the product after the emission of neutrons in the fission process. Since the distribution of protons in a given fission event occurs not later than the moment of scission, it is useful to estimate the number of neutrons which have been emitted by the fragment to produce the observed product mass. Neutron multiplicity values suggested by Terrell (21) and by Apalin et al. (22) show similar trends in the number of neutrons emitted as a function of product mass number; however, they are not identical. Although the error in estimation of neutron multiplicity increases the difficulty of physical interpretation of the radiochemical data, inclusion of these values in the calculations relates the data more directly to the fission process.

In Figure 11, the measured values of  $\sigma$  are plotted as a function of  $A'$ , the fragment mass before neutron emission, with values for complementary mass chains superimposed. Terrell's values for the number of neutrons emitted from fragments have been used to calculate  $A'$ .

The data now available show  $\sigma$  is not constant over the fission-product mass region, but insufficient data are available to predict unmeasured  $\sigma$  values. A physical explanation of the variation of  $\sigma$  with mass number is not apparent. The discontinuity of  $\sigma$  in the heavy-mass region lies near the 82-neutron shell in the fission fragment. The location of this shell with regard to the product mass number depends on the number of neutrons evaporated from the fragment.

The lowest value of  $\sigma$  reported is 0.29, calculated for the mass-136 chain by Strom (23) from fractional yields reported earlier by Katcoff (24), but the significance of this value is reduced by the uncertainty of the mass assignment for the iodine reported for this chain. For the mass-133 chain, a  $\sigma$  of  $0.45 \pm 0.03$  is reported by Strom et al. (20). For the mass-139 chain,  $\sigma$ , reported by Wahl et al. (7), is  $0.75 \pm \frac{0.14}{0.10}$ . The average fragment masses which result in products of mass 133-139 have been estimated using Terrell's values for the number of neutrons evaporated from a fragment (21), and also with Apalin's values for neutron multiplicities (22). The average number of neutrons in a fission fragment with the most probable charge ( $Z_p$ ) for the 133, 136, and 139 mass chains was estimated by subtracting the experimental  $Z_p$  value from the calculated fragment mass. Lack of data for the 137 and 138 mass chains prevents such calculations for these chains.

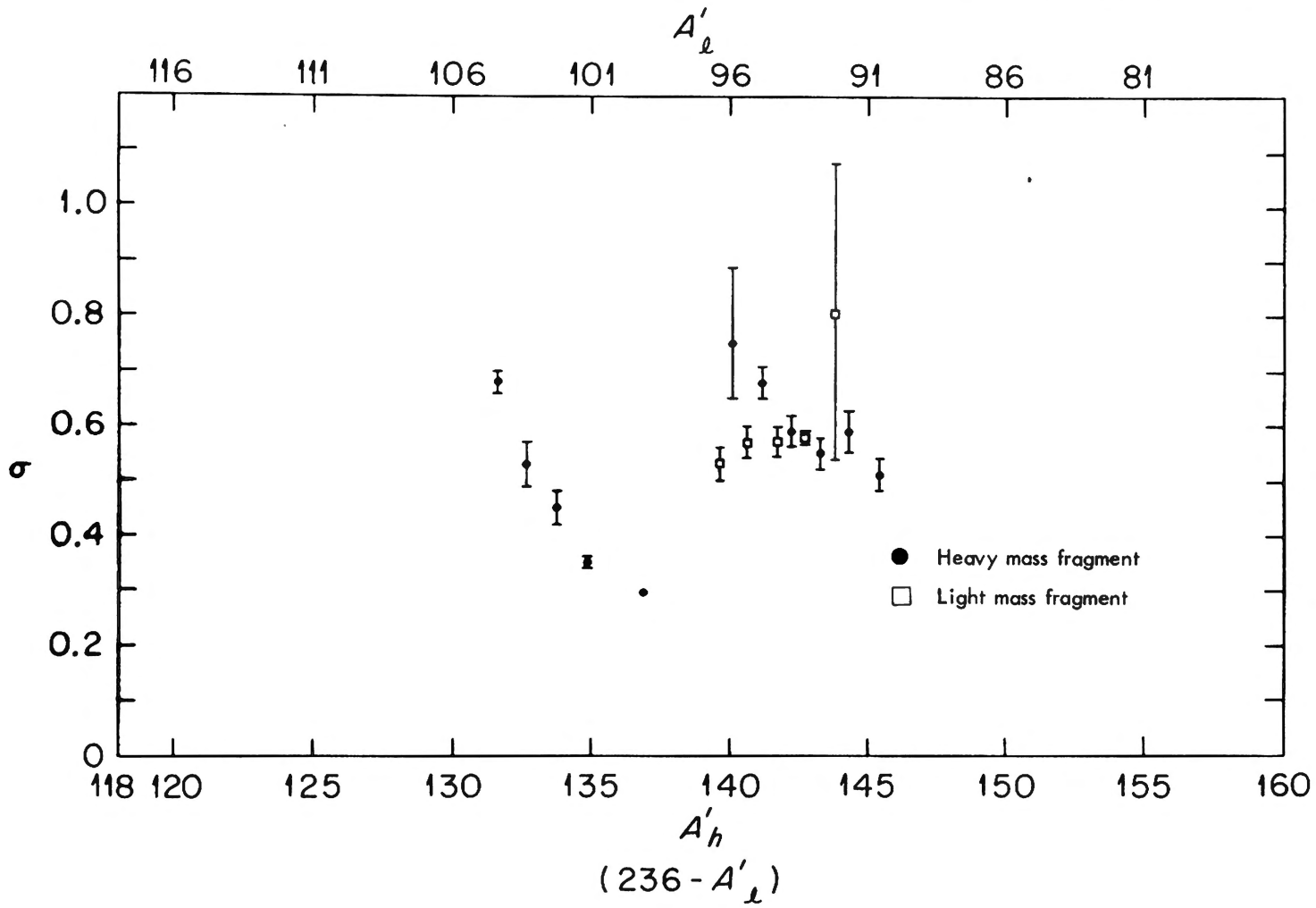


Figure 11. Known values of  $\sigma$  plotted as a function of  $A'$ .



Results are listed in Table IV. In spite of the uncertainties in neutron multiplicities and in  $Z_p$ , and the nature of the calculations, which result in non-integral  $Z_p$  and  $A'$  values, the proximity of the discontinuity to the 82-neutron shell is evident.

#### Variation of $Z_p$ With Mass Number

The postulates for the variation of  $Z_p$  with mass number have been described in Chapter I. A convenient method of presenting  $Z_p$  values as a function of fragment mass number is to plot the deviation from unchanged charge distribution (i. e., from products having the same neutron-proton ratio as the fissioning compound nucleus,  $^{236}\text{U}$ ). Figure 12 shows such a plot for measured values of  $Z_p$  in the 140-146 mass region; Apalin's values for the neutron multiplicities have been used to calculate  $A'$ . Measured  $Z_p$  values for complementary light-mass chains are superimposed by inverting the charge scale at the line representing unchanged charge distribution, since an increased density of charge in one fragment necessarily indicates a corresponding decrease in the complementary fragment. This plot shows the increased density of charge in the light fragment noted by Wolfsberg (8), who showed a deviation of  $\sim 0.6$  charge unit in favor of the light fragment, in thermal-neutron induced fission of  $^{235}\text{U}$  and  $^{233}\text{U}$ , and also in 14-MeV

TABLE IV

AVERAGE NUMBER OF NEUTRONS IN FISSION FRAGMENTS WITH  
THE MOST PROBABLE CHARGE (PRODUCT MASSES 133-139)

<u>A</u>	<u>Terrell's Neutron Multiplicities</u>		<u>Apalin's Neutron Multiplicities</u>		<u><math>\sigma</math></u>
	<u>A'</u>	<u><math>A' - Z_p</math></u>	<u>A'</u>	<u><math>A' - Z_p</math></u>	
133	133.7	82.1 $\pm$ 0.04	133.6	81.9 $\pm$ 0.04	0.45 $\pm$ 0.03
136	136.9	83.4	136.8	83.3	0.29
137	138.0	—	138.0	—	—
138	139.0	—	139.1	—	—
139	140.1	86.3 $\begin{matrix} + 0.14 \\ - 0.10 \end{matrix}$	140.28	86.5 $\begin{matrix} + 0.14 \\ - 0.10 \end{matrix}$	0.75 $\begin{matrix} + 0.14 \\ - 0.10 \end{matrix}$

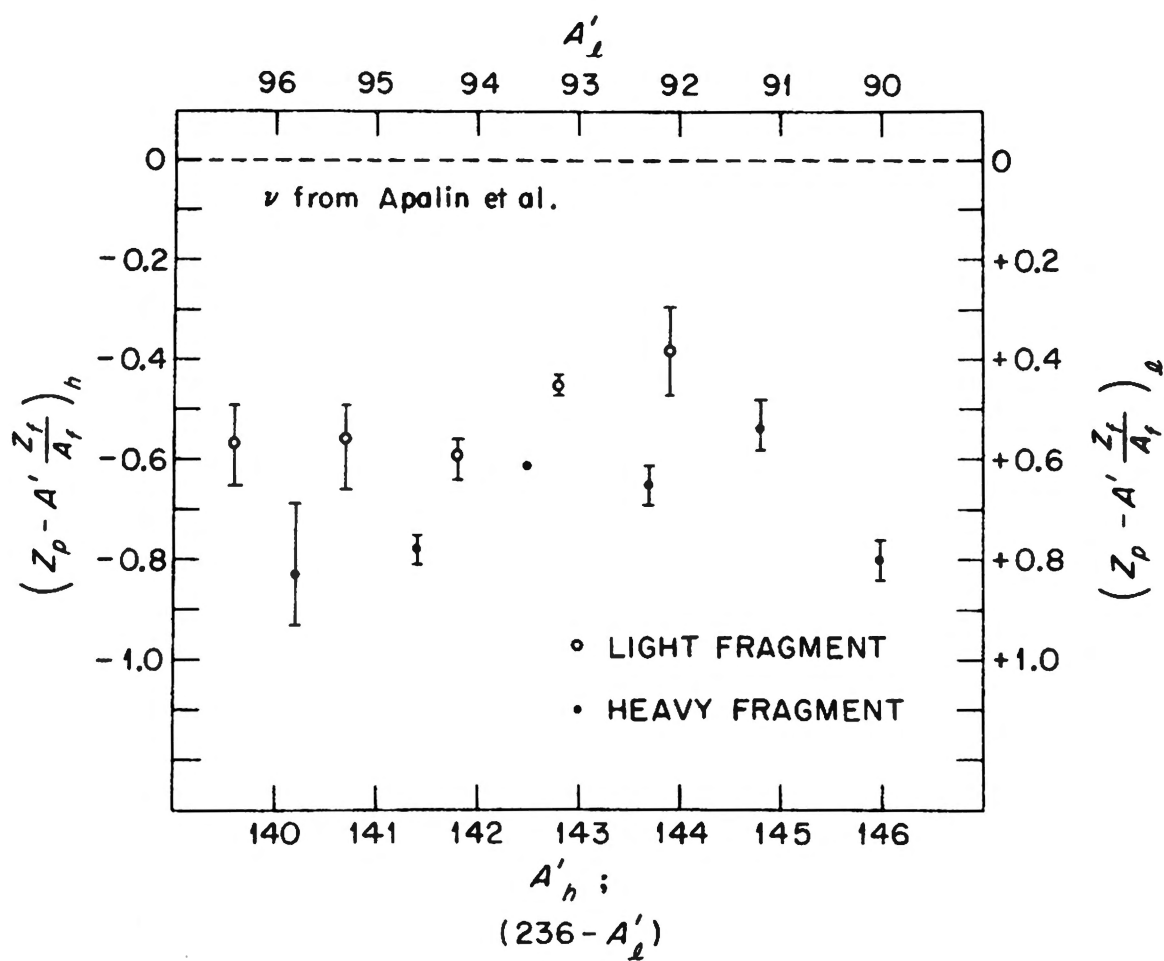


Figure 12.  $^{235}\text{U}(n_{\text{th}}, F)$  empirical  $Z_p$  values.

neutron induced fission of  $^{235}\text{U}$  and  $^{238}\text{U}$ . The deviation from unchanged charge distribution in the mass-144 chain is similar to the values previously measured in neighboring chains; it does not show a trend toward unchanged charge distribution.

Presently available data do not show whether this decreased density of charge continues for isobaric chains heavier than 144. Only three experimental fractional yields had been reported in these chains, previous to the present work. All of these values are of very small independent yields. For very small independent yields, errors in the  $\sigma$  assumed for the distribution lead to large errors in the calculated  $Z_p$ . For none of the masses above 144 has more than one fractional yield (providing an experimental observation of  $\sigma$ ) been measured. It is significant, then, that the  $Z_p$  reported here for the mass-144 chain shows the  $\sim 0.6$  charge-unit deviation in favor of the light fragment continuing; and it would be of interest to calculate  $Z_p$  for the mass-147 chain.

The postulates for predicting the variation of  $Z_p$  with fragment mass number diverge for the fission product masses above  $\sim 144$ . Here the postulate of equal charge displacement (ECD) predicts an increasing density of charge; Wahl's empirical relationship (7) also predicts an increasing density of charge, both still retaining a lower proton-to-

neutron ratio than  $^{236}\text{U}$ . Calculations using Niece's empirical  $\sigma$  function (9) result in a higher charge density for the heavy-mass fragments than that of the fissioning nucleus.

By use of the constant  $\sigma$  assumed and the  $Z_p$  predicted by Wahl et al., the fractional cumulative yields for the members of the mass-147 chain are predicted to be: lanthanum, 0.34; cerium, 0.95; and praseodymium, 0.9999. The predictions from Niece's  $\sigma$  function and  $Z_p$  values are: lanthanum, 0.0008; cerium, 0.20; and praseodymium, 0.95.

The value of the fraction of the 147 chain present as cerium at the mean irradiation time cannot be corrected exactly for the independent yield of  $^{147}\text{La}$ , since the half-life of this nuclide is unreported. This fraction,  $(0.96 \pm 0.063)$ , is, however, consistent with the yield predicted by Wahl's empirical function, and a half-life for  $^{147}\text{La}$  of  $\sim 2$  seconds. The measured fraction is inconsistent with Niece's prediction.

Because the  $Z_p$  values for this region were predicted by Niece from very small independent yields, these predictions are very sensitive to errors in estimating  $\sigma$ . The fact that the measured yield of  $^{147}\text{Ce}$  is consistent with Wahl's prediction and not with that of Niece suggests the decrease of  $\sigma$  with increasing mass number does not continue linearly in the heavy-mass region.

Half-Life of  $^{144}\text{Ba}$ 

In order to compare the half-life of  $^{144}\text{Ba}$ , found to be  $11.9 \pm 0.3$  seconds, with theoretical predictions, the energy available for the transition must be estimated. Viola (25) estimates 2.980 MeV for the transition to ground state  $^{144}\text{La}$ ; his predictions are based on nuclear decay energy systematics. An even-even isotope with 0 spin and even parity,  $^{144}\text{Ba}$  decays to odd-odd  $^{144}\text{La}$ . From Viola's estimate of the energy available and the measured half-life, this is an allowed transition. From shell model considerations, however, an odd parity state would be expected for  $^{144}\text{La}$ . If the transition is allowed, no parity change is predicted; for a forbidden transition (parity change) a half-life longer than that found would be expected.

A low-lying state of opposite parity in  $^{144}\text{Ba}$  or  $^{144}\text{La}$  would provide an explanation of the short half-life, but the uncertainty in the energy available for the transition makes the presently available evidence inconclusive.

## CHAPTER VI

### SUMMARY

In the mass-143 chain, a third fractional yield, the cumulative yield of  $^{143}\text{Ba}$ , has been measured and found to be  $0.875 \pm 0.040$ . This yield is consistent with the assumption of a Gaussian distribution for this chain;  $Z_p$  is  $55.92 \pm \frac{0.08}{0.10}$  and  $\sigma$  is  $0.59 \pm 0.04$ .

The fractional cumulative yield of  $^{144}\text{Ba}$  is  $0.773 \pm 0.035$ . In combination with the previously reported  $^{144}\text{Xe}$  yield, this measures the width of the nuclear charge distribution for the mass-144 chain;  $\sigma$  is  $0.51 \pm 0.03$ .  $Z_p$  for the mass-144 chain is  $56.11 \pm 0.04$ . The decrease in charge dispersion with increasing mass number, noted for isobaric chains of mass numbers 139 to 143, continues for mass 144. The decreased charge density, as compared to the fissioning compound nucleus, observed in other heavy-mass chains, also exists in the mass-144 chain.

The fractional cumulative yield of  $^{147}\text{Ce}$ , neglecting the small correction for the  $^{147}\text{La}$  independent yield, is  $0.963 \pm 0.063$ . Lack of other yield measurements in the mass-147 chain prevents calculation of a unique  $Z_p$  value or  $\sigma$  for this chain; the measured yield is not consistent with a  $\sigma$  as narrow as that predicted by a linear extrapolation of values measured for masses in the 139-144 mass region.

The half-life of  $^{144}\text{Ba}$  has been measured and found to be  $11.9 \pm 0.3$  seconds.



## BIBLIOGRAPHY

1. Halpern, I., Annual Reviews of Nuclear Science, (Annual Reviews, Inc., Palo Alto, California, 1959), p. 245.
2. Coryell, C. D., M. Kaplan, and R. D. Fink, Can. J. Chem. 39, 646 (1961).
3. Glendenin, L. E., C. D. Coryell, and R. R. Edwards, Radiochemical Studies: The Fission Products, edited by C. D. Coryell and N. Sugarman (McGraw-Hill Book Company, Inc., New York, 1951), National Nuclear Energy Series, Plutonium Project Record, Vol. 9, Div. IV, p. 489.
4. Pappas, A. C., Proceedings of the U. N. Conference on the Peaceful Uses of Atomic Energy 7, United Nations, Geneva, 1955, p. 19.
5. Fiedler, J., and G. Herrmann, Z. Naturforsch 18a, 533 (1963).
6. Blann, H. M., University of California Report URCL-9190, 1960 (unpublished).
7. Wahl, A. C., R. L. Ferguson, D. R. Nethaway, D. E. Troutner, and K. Wolfsberg, Phys. Rev. 126, 1112 (1962).
8. Wolfsberg, K., Phys. Rev. 137, B929 (1965).
9. Niece, L. H., Ph.D. Thesis, University of Missouri, 1965 (unpublished).
10. Herrmann, G., Habilitationsschrift, Universitat Mainz, 1964 (unpublished).
11. Bunney, L. R., E. C. Freiling, L. D. McIssac, and E. M. Scadden, Nucleonics 15, 81 (1957).
12. Rengan, K., and W. Meinke, Anal. Chem. 36, 157 (1964).
13. Rinehart, R. W., Anal. Chem. 26, 1820 (1954).
14. Hoffman, D. C., and W. R. Daniels, J. Inorg. Nucl. Chem. 26, 1769 (1964).

15. Youden, W. J., Statistical Methods for Chemists (John Wiley and Sons, Inc., New York, 1951).
16. Glendenin, L. E., K. F. Flynn, R. F. Buchanan, and E. P. Steinberg, Anal. Chem. 27, 59 (1955).
17. Bateman, H., Proc. Cambridge Phil. Soc. 15, 423 (1910).
18. Terrell, J., Phys. Rev. 108, 783 (1957).
19. Norris, A. E., Ph.D. thesis, Washington University, 1959 (unpublished).
20. Strom, P. O., D. L. Love, A. E. Greendale, A. A. Delucchi, D. Sam, and N. E. Ballou, U. S. Naval Radiological Defense Laboratory Technical Report USNRDL-TR-935, 1965 (unpublished).
21. Terrell, J., Phys. Rev. 127, 880 (1962).
22. Apalin, V. F., Y. N. Gritsyuk, I. E. Kutikov, V. I. Lebedev, and L. A. Mikaelyan, Nucl. Phys. 55, 249 (1964) and Soviet Physics JETP 19, 810 (1964).
23. Strom, P. O., private communication to R. L. Ferguson, (1965).
24. Katcoff, S., Nucleonics 18, No. 11, p. 201 (1960).
25. Viola, V. E., Jr. (private communication), 1966.

## VITA

The author was born February 28, 1930, at Omaha, Nebraska, and attended public schools in that state. She was awarded the B.S. degree cum laude by the Nebraska State College at Kearney in 1951. After graduation, she taught in the high school at Blue Hill, Nebraska for two years. She was married to James J. Runnalls in May, 1952. They are the parents of two children, Andrea and Christopher.

The author entered Mankato State College at Mankato, Minnesota as a graduate student in chemistry in 1961. She was employed as a graduate assistant during the 1962-63 school year, and was graduated with the M.S. degree in June, 1963. She entered the University of Missouri in June, 1963, and was employed as a graduate assistant in chemistry there during the 1963-64 and 1964-65 school years. She received an American Association of University Women fellowship in July, 1965, and has remained at the University of Missouri since that time.

The undersigned, appointed by the Dean of the Graduate Faculty, have  
examined a thesis entitled

YIELDS FROM HIGHLY ASYMMETRIC FISSION:  
FRACTIONAL CUMULATIVE YIELDS OF  
 $^{143}\text{Ba}$ ,  $^{144}\text{Ba}$ , AND  $^{147}\text{Ce}$  FROM  
THERMAL-NEUTRON INDUCED  
FISSION OF  $^{235}\text{U}$

presented by . Nelva Gross Runnalls

a candidate for the degree of Doctor of Philosophy

and hereby certify that in their opinion it is worthy of acceptance.

David E. Iroutner  
Robert R. Kuntz  
Guy Schupp

University of Missouri - Columbia  
ELL C70441  
QD31.Y1966 R8



010-003519295

QD  
31  
.Y1966  
.R8  
C70441

University Libraries  
University of Missouri

### Digitization Information Page

Local identifier                      DTD-Runnalls1966

#### Source information

Format                                  Book  
Content type                          Text  
Source ID                              010-003519295  
Notes

#### Capture information

Date captured                        January 2021  
Scanner manufacturer                BookDrive  
Scanner model                         Mark 2  
Scanning system software          BookDrive Capture  
Color settings                         24 bit color  
File types                              Raw  
Notes

#### Derivatives - Access copy

Compression                         Tiff: LZW compression  
Editing software                      Adobe Photoshop CC  
Resolution                              600 dpi  
Color                                    grayscale  
File types                              pdf created from tiffs  
Notes                                    Images cropped, straightened, brightened  
Canvas size: 8.5" x 11"